Unraveling the Complex Hydrogen Bonding of a Dual-Functionality Proton Conductor Using Ultrafast Magic Angle Spinning NMR

Jason W. Traer,[†] Enzo Montoneri,[‡] Ago Samoson,[§] Jaan Past,[§] Tiit Tuherm,[§] and Gillian R. Goward*,[†]

Department of Chemistry, McMaster University, 1280 Main Street West, Hamilton, ON, L8S 4M1, Canada, Dipartimento di Chimica Generale ed Organica Applicata, Università di Torino, C. M. D'Azeglio 48, 10126 Torino, Italy, and National Institute Of Chemical Physics and Biophysics, Akadeemia tee 23, 12618 Tallinn, Estonia

Received March 2, 2006. Revised Manuscript Received July 5, 2006

Hydrogen bonding plays a critical role in proton-conducting polymers, as it provides the network necessary for structural (Grotthus mechanism) diffusion. This network must be both pervasive and dynamic in order for long-range proton transport to be achieved. The structural motifs must be understood, even in amorphous materials, and moreover, the lattice energies in the structure must be low enough to allow rearrangement and mobility. To this end, a novel proton-conducting candidate, 1,10-(1-*H*-imidazol-5-yl)decanephosphonic acid and its HBr doped counterpart are considered from the molecular level as potential proton-conducting membranes. The use of high-resolution solid-state ^{1}H NMR to elucidate structure and dynamics of such systems is highlighted in this material. We compare our molecular-level results to macroscopic probes of proton transport in related polymers, achieved using impedance spectroscopy.

Introduction

The ongoing search for inexpensive, durable proton-conducting membranes for fuel cell applications has motivated the development of several novel polymeric systems in recent years.[1] Many of these involve sulfonation of aromatic polymers, creating polymers that mimic the proton-transport mechanisms of the perfluorinated ionomer, Nafion, in which high humidity is important.[2] To increase the operating temperature of fuel cells, membranes are needed which are able to operate under moderate temperatures (∼150 °C). To achieve this, polyelectrolytes which conduct independent of high humidification are required. The closest competitor to Nafion are the phosphoric acid-doped polybenzimidazoles[3] and polyphosphazenes.[4] While these and related aromatic polymer systems have received a lot of press, the high molar ratio of acid to polymer makes such systems susceptible to acid leaching, and thus not ideal. The synthetic challenge is to create a covalently tethered proton solvent which will allow proton conductivity through a Grotthus (structural diffusion) mechanism at a rate which can compete with proton transport in a highly humid environment. This is a lofty goal, and as yet, no material has been prepared which can meet these demands in the absence of significant hydration or an acid dopant.

To achieve a liquid-free membrane candidate, heterocycles tethered to polymer backbones are targeted. Heterocycles themselves, including imidazole, fluorinated imidazole, and imidazolium salts, have been studied extensively to characterize the energetically costly steps in the Grotthus mechanism.[5] Ethylene backbones with imidazole or vinazene functional units, as well as imidazole rings tethered to ethylene oxide, styrene, or siloxane chains, have been prepared and characterized.[6] Polymers which incorporate imidazole groups complexed with free phosphonic acid, or copolymerized as 4-vinylimidazole plus vinylphosphonic acid, have also been considered.[7,8] Our study focuses on a

[†] McMaster University.
[‡] Università di Torino.
[§] National Institute of Chemical Physics and Biophysics, Tallinn.

(1) Schuster, M.; Rager, T.; Noda, A.; Kreuer, K. D.; Maier. J. *Fuel Cell* **2005**, *3* 355−366.
(2) Asano, N.; Aoki, M.; Suzuki, S.; Miyatake, K.; Uchida, H.; Watanabe, M. *J. Am. Chem. Soc.* **2006**, *128*, 1762−1769.
(3) (a) Asensio, J. A.; Gomez-Romero, P. *Fuel Cell* **2005**, *3*, 336−344. (b) Li, Q.; He, R.; Jensen, J. O.; Bjerrum, N. J. *Fuel Cells* **2004**, *4*, 147−159. (c) Qingfeng, L.; Hjuler, H. A.; Bjerrum, N. J. *J. Appl. Electrochem.* **2001**, *31*, 773−779. (d) Gourdoupi, N.; Andreopoulou, A. K.; Deimede, V.; Kallitsis, J. K. *Chem. Mater.* **2003**, *15*, 5044−5050. (e) Xiao, L.; Zhang, H.; Scanlon, E.; Ramanathan, L. S.; Choe, E. W.; Rogers, D.; Apple, T.; Benicewicz, B. C. *Chem. Mater.* **2005**, *17*, 5328−5333.
(4) Dotelli, G.; Gallazzi, M. C.; Perfetti, G.; Montoneri, E. *Solid State Ionics* **2005**, *176*, 2819−2827.
(5) (a) Hickman, B. S.; Mascal, M.; Titman, J. J.; Wood, I. G. *J. Am. Chem. Soc.* **1999**, *121*, 11486−11490. (b) Munch, W.; Kreuer, K. D.; Silvestri, W.; Maier, J.; Seifert, G. *Solid State Ionics* **2001**, *145*, 437−443. (c) Goward, G. R.; Fischbach, I.; Saalwachter, K.; Spiess, H. W. *J. Phys. Chem. B* **2004**, *108*, 18500−18508. (d) Deng, W.-Q.; Molinero, V.; Goddard, W. A., III. *J. Am. Chem. Soc.* **2004**, *126*, 15644−15645.
(6) (a) Pu, H.; Meyer, W. H.; Wegner, G. *Macromol. Chem. Phys.* **2001**, *202*, 1478−1482. (b) Densmore, C.; Rasmussen, P.; Goward, G. R. *Macromolecules* **2005**, *38*, 416−421. (c) Schuster, M.; Meyer, W. H.; Wegner, G.; Herz, H. G.; Ise, M.; Schuster, M.; Kreuer, K. D.; Maier, J. *Solid State Ionics* **2001**, *145*, 85−92. (d) Goward, G. R.; Schuster, M. F. H.; Sebastiani, D.; Schnell, I.; Spiess, H. W. *J. Phys. Chem. B* **2002**, *106*, 9323−9334. (e) Schuster, M. F. H.; Meyer, W. H.; Schuster, M.; Kreuer, K. D. *Chem. Mater.* **2004**, *16*, 329−337. (f) Benhabbour, S. R.; Scharfenberger, G.; Meyer, W.; Goward, G. R. *Chem. Mater.* **2005**, *17*, 1605−1612.
(7) Bozkurt, A.; Meyer, W. H. *Solid State Ionics* **2001**, *138*, 259−265.
(8) Bozkurt, A.; Meyer, W. H.; Gutmann, J.; Wegner, G. *Solid State Ionics* **2003**, *164*, 169−176.

10.1021/cm060514i CCC: $33.50
Published on Web 09/06/2006

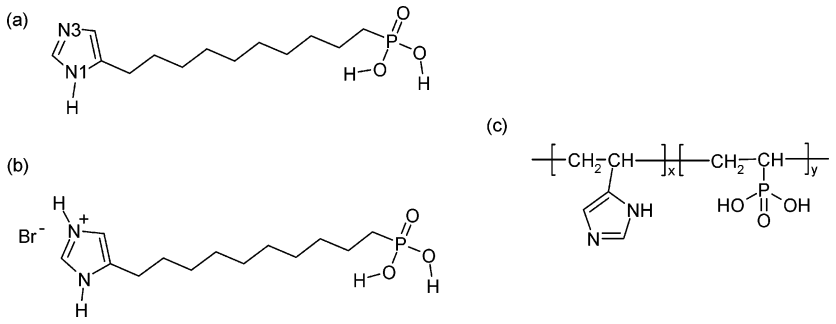

Figure 1. Molecular structures of (a) 1,10-(1-*H*-imidazol-5-yl)decanephosphonic acid (Imi-d-PA) and (b) 1,10-(1-*H*imidazol-5-yl)decanephosphonic acid HBr complex, and (c) poly(VPA-*co*-4-VIm).[8]

novel, dual-functionality molecule, 1,10-(1-*H*-imidazol-5-yl)-decanephosphonic acid,[9] which incorporates both imidazole and phosphonic acid groups, covalently tethered via a flexible decane backbone. This material (hereto called Imi-d-PA) was synthesized by coauthors in Italy and is characterized here. Critical to the performance of this new material are both its structure and its proton dynamics. These fundamental properties will govern the mechanism of proton transport and are therefore important to further materials development. The questions we answer here are, first, what is the solid-state structure of this material, and second, is that structure conducive to long-range proton transport? For comparison, we include the HBr complex of Imi-d-PA, as its propensity for efficient proton conductivity surpasses its undoped counterpart. The structures of the molecules of interest are shown in Figure 1. The structure of a related copolymer, formed of vinylphosphonic acid and 4-vinylimidazole, poly-(VPA-*co*-4-VIm), is included as Figure 1c. This polymer is used for comparison since conductivity data are available for this material.[8] The first notable feature of Imi-d-PA is the number of potential hydrogen-bonding sites: two donors and three acceptors. This may result in a rearrangeable hydrogen bonding structure. Second, the flexible backbone may provide local mobility, facilitating ring reorientation. These possibilities are investigated using advanced solid-state NMR methods.

Methodology

Solid-state NMR is a highly effective tool for probing structure and dynamics in amorphous hydrogen-bonded materials.[10] More specifically, NMR techniques have been used to characterize many features of proton-conducting membranes for fuel cell applications, including ^{13}C NMR of backbone dynamics,[11] ^{31}P NMR of phosphoric acid dopants,[12] ^{1}H NMR of proton dynamics in hydrated Nafion and S-PEEK membranes,[13] and ^{1}H NMR microscopy of water within fuel cells themselves.[14] Here, we establish a packing motif for Imi-d-PA using a series of homonuclear and heteronuclear correlation experiments to ascertain the hydrogen-bonding structure based on the observed couplings. High-resolution solid-state ^{1}H NMR spectra are acquired under fast magic angle spinning conditions, up to 60 kHz.[15,16] These conditions are sufficient to achieve excellent spectral resolution in the hydrogen-bonding region of the spectrum. $^{1}H-^{1}H$ double quantum filtered (DQF) 2D spectra are used to assign through-space (dipolar) couplings within the hydrogen-bonded network.[10,17,18] For protons which are rigid on the time scale of the experiment ($\sim$1 rotor period, τ_r), their dipolar couplings are not motionally averaged, and any correlations to neighboring protons are observed through correlations in the double quantum dimension of the 2D spectrum. As a first test, the relative mobilities of protons can be deduced from the response of the material to a 1D ^{1}H MAS versus a 1D ^{1}H DQF sequence. Resonances which are removed (filtered) by the latter are considered mobile in the time frame of the pulse sequence.[6d]

The $^{1}H-^{1}H$ 2D DQF data are correlated with heteronuclear $^{1}H-^{13}C$, $^{1}H-^{31}P$, and $^{1}H-^{15}N$ spectra acquired under fast magic angle spinning and variable contact times. The latter experiments are driven by dipolar coupling strengths, which provide the magnetization transfer from the abundant (^{1}H) spins to the heteronuclei. In this way, the combination of techniques allows for a jigsaw puzzle-solving approach to linking up the pieces of the molecules into a cohesive picture of the structure, based on the most general assignment of the constraints provided by the experimental data. Overall, a complete picture of the local packing is obtained. This is similar to the approach used for solving complex protein structures using NMR spectroscopy. Here we have in this case additional challenges due to the lack of isotopic labeling or enrichment, and the lack of long-range crystallinity in the sample. Variable temperature ^{1}H NMR studies are used to characterize proton mobility in both pristine and HBr-doped materials.

(9) Montoneri, E.; Gallazzi, M. C.; Bertarelli, C.; Gobetto, R.; Salassa, L. *Phosphorus, Sulfur, Silicon* **2004**, *179*, 1737−1755.
(10) (a) Goward, G. R.; Sebastiani, D.; Schnell, I.; Spiess, H. W.; Kim, H.-D.; Ishida, H. *J. Am. Chem. Soc.* **2003**, *125*, 5792−5800. (b) Brown, S. P.; Schnell, I.; Brand, J. D.; Mullen, K.; Spiess, H. W. *J. Mol. Struct.* **2000**, *521*, 179−195.
(11) Liu, S.-F.; Schmidt-Rohr, K. *Macromolecules* **2001,** *34*, 8416−8418.
(12) Hughes, C. E.; Haufe, S.; Angerstein, B.; Kalim, R.; Maehr, U.; Reiche, A.; Baldus, M. *J. Phys. Chem. B* **2004,** *108*, 13626−13631.
(13) (a) Cherry, B. R.; Fujimoto, C. H.; Cornelius, C. J.; Alam, T. M. *Macromolecules* **2005**, *38*, 1201−1206. (b) Ye, G.; Janzen, N.; Goward, G. R. *Macromolecules* **2006**, *39*, 3283−3290.
(14) Feindel, K. W.; LaRocque, P.-A. L.; Starke, D.; Bergens, S. H.; Wasylishen, R. E. *J. Am. Chem. Soc.* **2004**, *126*, 11436−11437.
(15) (a) Samoson, A.; Tuherm, T.; Past, J. *Chem. Phys. Lett.* **2002**, *365*, 292−299. (b)Samoson, A.; Tuherm, T.; Past, J.; Reinhold, A.; Anupõld, T.; Heinmaa, I. *Top. Curr. Chem.* **2005**, *246 (New Techniques in Solid-State NMR)*, 15−31.
(16) Ernst, M.; Samoson, A.; Meier, B. H. *Chem. Phys. Lett.* **2001**, *348*, 293−302.
(17) Schnell, I.; Spiess, H. W. *J. Magn. Reson.* **2001**, *151*, 153−227.
(18) Brown, S. P.; Spiess, H. W. *Chem. Rev.* **2001**, *101*, 4125−4155.

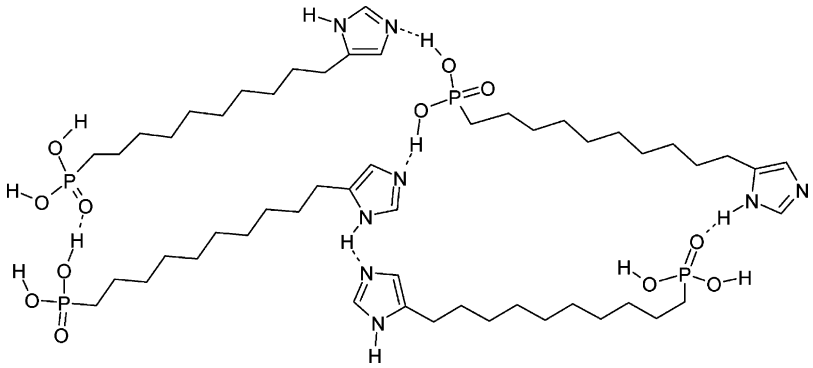

Figure 2. Proposed solid-state packing motif for hydrogen bonding in Imi-d-PA, including asymmetric bonding at the imidazole rings. This proposed structure will be verified using solid-state NMR data and tested for proton mobility within the extensive hydrogen-bonding network using variable temperature NMR studies.

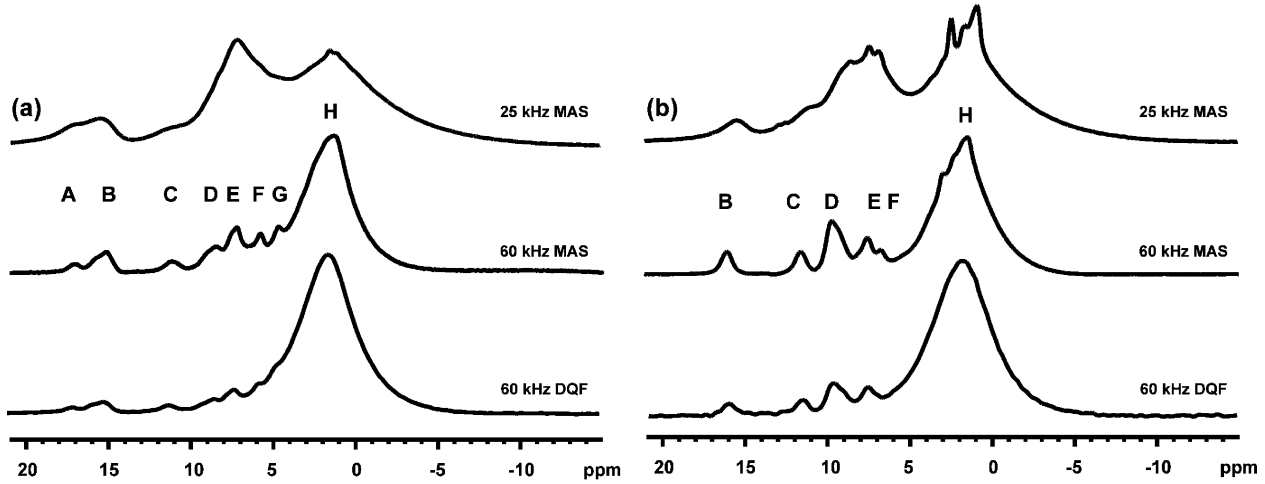

Figure 3. Solid-state ^{1}H MAS NMR spectra of (a) Imi-d-PA and (b) Imi-d-PA-HBr. The top spectra are acquired at 25 kHz MAS on a 500 MHz AV spectrometer, using a 2.5 mm outer diameter rotor, containing ~10 mg of material. The middle spectra are acquired at 60 kHz MAS on a 600 MHz AV spectrometer, using a 1.1 mm outer diameter rotor, containing <5 mg of material. The bottom spectra are acquired at 60 kHz MAS, using the rotor-synchronized double quantum filtering sequence. Proton resonances are labeled and classed: A−D represent hydrogen-bonded protons, E−G represent aromatic protons, and H represents aliphatic protons.

Results and Discussion

Applying the least number of constraints to the system, we begin with a static, asymmetric packing around the imidazole rings. The structure is shown in Figure 2, including all possible hydrogen-bonding contacts. First we show that the data acquired supports the existence of this complex hydrogen bonding structure. Second, we probe whether this structure is capable of transferring protons within the hydrogen bonded network, whether by phosphonate rotation or imidazole ring flipping.

Figure 3a shows the ^{1}H solid-state NMR spectrum of Imi-d-PA, acquired under 60 kHz MAS. Relative to a solution-state spectrum in which the hydrogen-bonded protons are invisible due to rapid exchange, the solid-state MAS spectrum includes many resonances in the hydrogen-bonding region, indicating immediately a complex packing structure. The assignment of these resonances forms the crux of the argument for the hydrogen-bonding motif. At this point, the proton resonances, labeled A−H, are generally classed as follows. Resonance H is assigned to the methylene protons of the decane backbone. We note that the line width of this resonance is extremely sensitive to spinning speed, as illustrated in the difference between the top spectrum and middle spectrum of Figure 3a, where the aliphatic line widths are 4.4 kHz at 25 kHz MAS and 1.3 kHz at 60 kHz MAS, respectively.[19,20] This is due to the strength of the homonuclear dipolar coupling between protons bound to the same carbon. The dramatic narrowing of this signal by MAS at 60 kHz is critical to the success of this study. Without this, the resonance would overlap the structurally significant resonances in the aromatic and hydrogen-bonding regions, making a complete assignment impossible. Resonances A−D are attributed to hydrogen-bonded protons, and resonances E−G are attributed to aromatic protons at this point. This assignment is based on the chemical shift ranges of the peaks in question (H-bonding from 18 to 9 ppm, aromatic from 5 to 8 ppm) and will be supported or disproved by the following studies.

The bottom spectrum in Figure 3a shows the 1D DQF spectrum acquired for Imi-d-PA at 60 kHz. From this we

(19) Note that the heating effects induced by spinning have been calibrated to be less than 15 °C on the 1.1 mm probe, which is fitted with a gas cooling line, and 10 °C on the 2.5 mm probe; thus, the spectra are acquired at sample temperatures within 5 °C of each other, and the line narrowing is attributable to MAS averaging alone. Also, all sample temperatures reported for the 2.5 mm probe (25 kHz MAS) have been calibrated using a $SmSn_2O_7$ chemical shift thermometer.

(20) (a) Langer, B.; Schnell, I.; Spiess H. W.; Grimmer, A.-R *J. Magn. Reson.* **1999**, *138*, 182. (b) Grimmer, A.-R.; Kretschmer, A.; Cajipe, V. B. *Magn. Reson. Chem.* **1997**, *35*, 86.

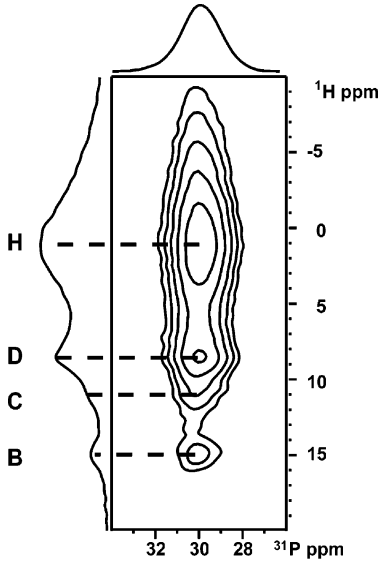

Figure 4. 2D ^{1}H−^{31}P heteronuclear correlation spectra acquired under 25 kHz MAS, at 500 MHz (^{1}H resonance frequency), using cross polarization contact times of 3 ms. Correlations to protons are indicated and match with the labeling of the ^{1}H MAS NMR spectrum from Figure 3.

can directly conclude that none of the protons are mobile at this temperature, on the time scale of the experiment ($1\tau_r <$ 20 μs), as all proton resonances observed in the 1D MAS spectrum are also observed in the 1D DQF spectrum. The same is true of the HBr complex at this sample temperature, where the analogous spectra are shown in Figure 3b. In the solid state, the imidazole rings exist as imidazolium. The imidazolium cation exists because the basic site in the solid state is protonated and forms a hydrogen bond. The acidic site of the imidazole will also form a hydrogen bond with another basic site. Formation of two hydrogen bonds will spread the positive charge over the imidazole ring, while a net negative charge can be attributed to the phosphate. The Imi-d-PA is already zwitterionic in the solid state because the acidic and basic ends of the molecule will form hydrogen bonds. Therefore, relatively small changes in the ^{1}H spectrum are observed upon addition of complexing HBr.

Heteronuclear ^{1}H−^{13}P 2D correlation spectra are utilized to distinguish which hydrogen-bonding moieties include the phosphate group and which do not. An example spectrum is shown in Figure 4. A single ^{31}P resonance is observed, consistent with an earlier report of the 1D ^{31}P spectrum of this compound. There are correlations to four types of protons. The strongest, but least informative, is the ^{31}P−H correlation, which is strong due to the large number of methylene protons contributing to this resonance. More informative are the correlations to protons B, C, and D. B and D are directly visible as maxima in the contour map, whereas C is evident upon detailed inspection of the slices making up the map. The projection shown on the left of the spectrum gives a clear assignment of the proton resonances. Most important in this data set is the absence of a correlation between proton resonance A and the phosphorus site. This was true regardless of the contact time for the cross polarization step of the experiment. Therefore, three of the H-bonded resonances can be attributed to hydrogen bonds involving the phosphate group, whereas resonance A is assigned to a hydrogen bond between the two imidazole

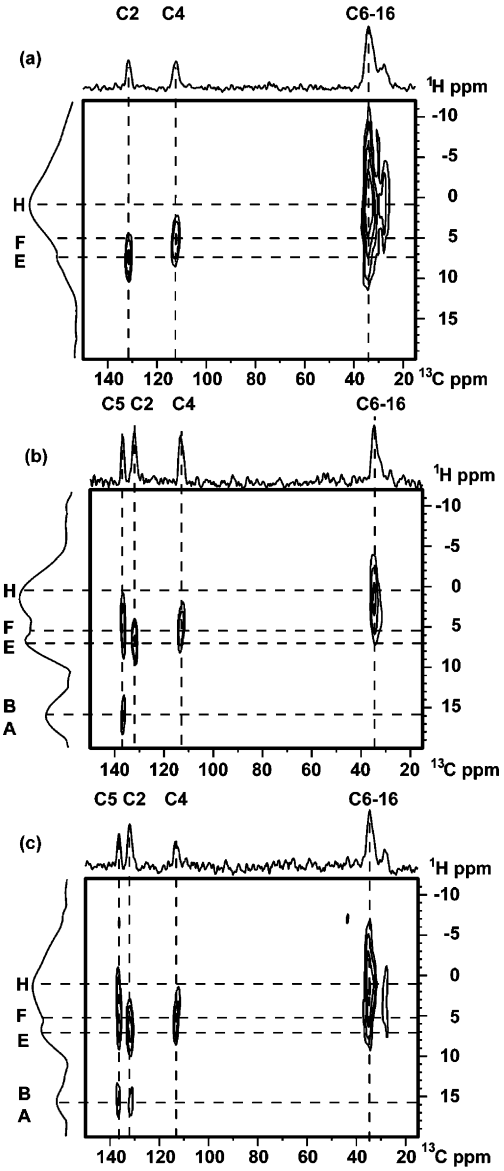

Figure 5. 2D ^{1}H−^{13}C heteronuclear correlation spectra acquired under 25 kHz MAS, at 500 MHz (^{1}H resonance frequency), using cross polarization contact times of (a) 0.5 ms, (b), 3 ms, and (c) 6 ms. In all cases, contours are calculated from 10% of the maximum intensity, using an increment of 1.5 over 18 contours. The inset shows the molecular structure of Imi-d-PA, with the carbons labeled numerically. Corresponding ^{13}C assignments are given on each of the spectra. Correlations to protons are indicated and match with the labeling of the ^{1}H MAS NMR spectrum from Figure 3.

rings. Further confirmation of this assignment is available from the ^{1}H−^{13}C 2D correlation spectra.

The ^{1}H−^{13}C 2D correlation spectra are shown in Figure 5. As the contact time for the cross polarization step is increased, the distance between the protons and the carbon nuclei contributing to the spectrum increases. Through a methodical examination of these spectra, an assignment of the ^{13}C chemical shifts and a confirmation of the assignment of proton resonance A are obtained. At the shortest contact time of 0.5 ms, Figure 5a, contacts are observed for directly bonded C−H units, including the decane backbone, and the aromatic C−H groups. Lengthening the contact time to 3 ms, and then to 6 ms, allows us to observe all the ^{1}H−^{13}C contacts, including the important correlations between the aromatic carbons and the hydrogen-bonded resonance A. The former is consistent with our earlier assignment of resonance

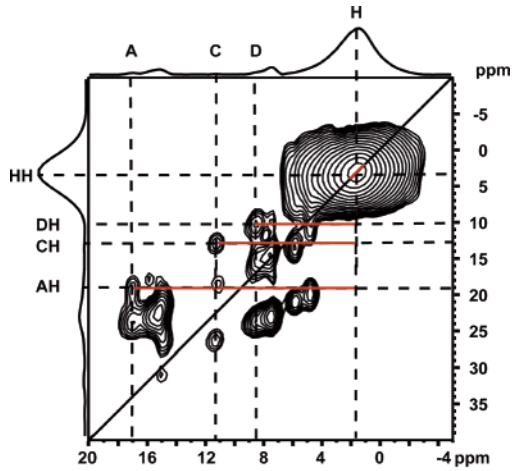

Figure 6. Homonuclear ^{1}H 2D double quantum filtered NMR spectrum of Imi-d-PA acquired at 60 kHz MAS, with correlations to aliphatic resonance H labeled.

A to a hydrogen bond involving two imidazole rings, and no contact to the phosphonate. Moreover, the relative strengths of the ^{1}H−^{13}C couplings of C2 and C5 to proton resonance A allow us to further assign the orientation of N1 and N3 unequivocally. As N1 is covalently bonded to its proton, it provides a shorter distance and stronger dipolar coupling between its proton and both C2 and C5, whereas the longer N3---H distance results in a weaker coupling of this proton to carbons on its imidazole ring, such that no correlation to C4 is observed. These spectra therefore provide strong confirmation of the asymmetric hydrogen bonding around the imidazole ring.

After the correlations between protons and their neighboring heavy atoms are established, the next data to consider are the correlations among the protons themselves. Homonuclear ^{1}H 2D double quantum filtered (DQF) spectra provide these critical details of the packing structure. Figure 6 shows the 2D DQF spectrum of Imi-d-PA acquired at 60 kHz MAS. The spectrum was acquired using the Back to Back, or BaBa, pulse sequence, which is known to be a robust sequence under fast magic angle spinning.[17,18] Figure 6 shows the full spectrum, including the strong self-correlation between the CH_2 protons, on the diagonal in the top right of the spectrum. Figure 7 shows the hydrogen-bonding region of the same spectrum. To briefly summarize the interpretations of these spectra, the resonances in the direct (single quantum) dimension match with those in the one-dimensional spectrum (Figure 3a), whereas the resonances in the indirect (double quantum) dimension occur at the sum of the single quantum frequencies of the dipolar coupled pair. Thus, correlations between like protons are found on the diagonal and correlations between unlike protons occur on either side of the diagonal, at the corresponding double quantum frequency.

The interpretation of this spectrum is systematic, and yet involved. The assignment resulting from these spectra confirms that four types of hydrogen bonds are found in the packing arrangement of Imi-d-PA, consistent with the most general arrangement with fewest constraints. To establish the assignment, we analyzed each proton resonance individually. Contacts to the backbone protons are shown in Figure 6 only, for simplicity. The short contacts attributed to each resonance are shown in Figure 7, with the accompanying structures below.

Dipolar coupling partners for proton resonance A include a correlation to the aliphatic backbone (A−H) and to the aromatic resonance (A−E). These correlations, together with the absence of resonance in the ^{1}H−^{31}P CPMAS spectrum, support the assignment of a hydrogen bond between imidazole rings with the nitrogen at the first position (N1) donating a proton to a nitrogen atom in the tertiary position (N3) on another imidazole ring (N1−H···N3).

Proton resonance C at 11 ppm is nicely separated from the neighboring resonances and is involved in three dipolar coupling contacts. The C−H contact to the decane chain and C−E contact to the aromatic ring locate the proton on the imidazole ring, while the strong C−B contact gives a clear intramolecular contact to an adjacent hydrogen bond on the phosphonate group. This, together with the ^{1}H−^{31}P correlation for this resonance, provides the assignment of this proton to a hydrogen bond from the phosphonate group to an imidazole ring.

In contrast to resonance C, proton resonance B has many dipolar coupling partners. Nevertheless, a full assignment is obtained (shown in Figure 7b), including in particular the B−C and B−D resonances, which indicate correlations between the B proton and the other hydrogen-bonded protons on the same phosphonate group. This intriguing correlation is further discussed below. Further, the relative strengths of the B and C correlations allow us to localize proton C on the N1 site in the imidazole ring. The doubly bonded oxygen (O═P) of the phosphonic acid is acting as the accepting site for the hydrogen bond. The N1 proton is a weakly acidic site while the double-bonded oxygen (O═P) is a weakly basic site. The proton resonance G has a very similar chemical shift to F. It is well-resolved as a B−G correlation. We tentatively assign resonance G to a ring-current effect on the neighborhing protons; however, this is somewhat unclear. The lack of other couplings to this resonance (hetero or homonuclear) preclude a more exact assignment. The weak B−B autocorrelation is attributed to a long-range coupling to a chemically equivalent, B proton through packing effects.

Proton resonance D is relatively simple to consider, as it has few contacts. The contact to the decane backbone (D−H) is clear. Particularly informative are the diagonal resonance D−D and the D−B coupling. The former represents a contact to a proton in an identical environment, which is satisfied by a dipolar coupling to the equivalent proton on its phosphonate hydrogen-bonding partner, as illustrated in Figure 7d. The latter, B−D coupling, indicates a correlation to an adjacent hydrogen-bonded proton on the same phosphonate group. This resonance is unique, as it represents a bifurcated hydrogen-bonding oxygen, as found in crystalline ice. Illustrated in Figure 7d, this oxygen is involved in hydrogen bonds to both an imidazole ring, at the N1 site, and the oxygen on a neighborhing phosphonate group. Supporting evidence for this type of hydrogen-bonding arrangement has been found in crystallographic studies of a

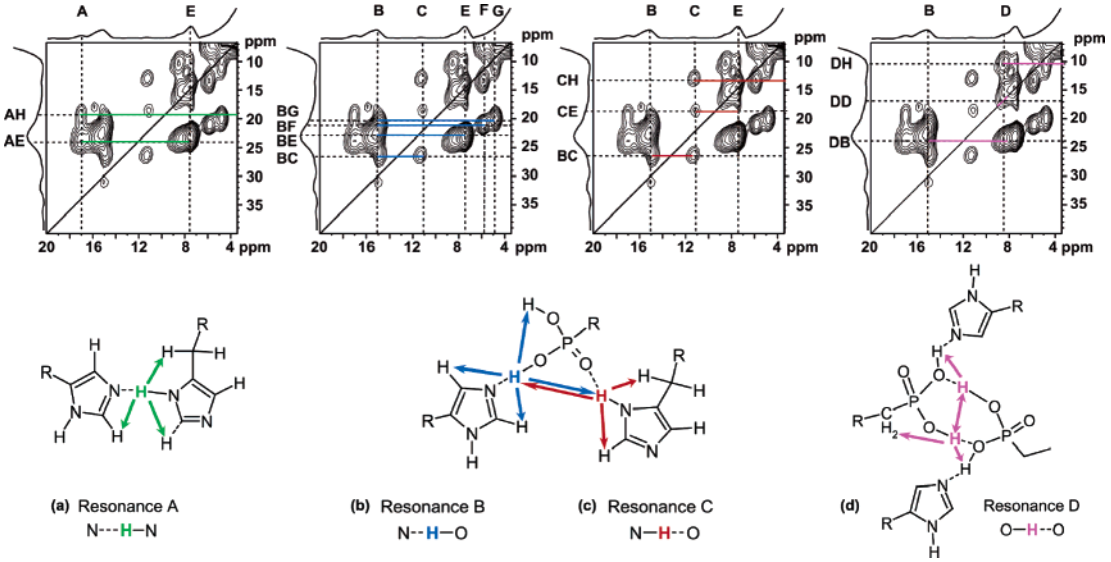

Figure 7. ^{1}H 2D DQF NMR of Imi-d-PA acquired at 60 kHz MAS, highlighting the hydrogen-bonding region, with all dipolar coupled pairs labeled. Dipolar couplings with individual proton resonance and the accompanying structural assignment are shown in (a) for proton A, (b) for proton B, (c) for proton C, and (d) for proton D.

related salt, benzimidazolium methylphosphonate (data not shown).

It is important to note at this point that our results provide a more accurate structural motif than an earlier proposed structure for Imi-d-PA.[9] The earlier structure was based primarily on the observation of a single ^{15}N resonance, from which the assumption of a symmetric hydrogen bonding around the imidazole rings was made. Upon further inspection, the line width of this ^{15}N resonance (12 ppm) was certainly large enough to span two poorly resolved nitrogen resonances, as is seen in the related case of crystalline benzimidazolium methylphosphonate, where the two ^{15}N resonances in the salt are separated by only 8 ppm at 11.7 T (data not shown). Without the solid-state ^{1}H NMR data, and 2D heteronuclear NMR spectra for Imi-d-PA, this earlier structure was consistent with the experimental data to that point. However, the data obtained here give a complete picture of the many proton local environments, and a full assignment of the hydrogen-bonding structure.

This complete assignment of the hydrogen-bonding motifs in Imi-d-PA provides an impression of the complexity of the network available for proton transport in this molecule and matches in detail the structure proposed at the outset in Figure 2. The diversity of hydrogen bonding strengths, ascertained from the varying degrees of acidity of basicity of the donor and acceptor sites, would seem to provide an obvious conduit for a dynamic and rearrangeable network. After our structural investigations, variable temperature ^{1}H NMR studies were used to probe proton dynamics. Before consideration of the ^{1}H NMR, however, the results of thermal analysis of both Imi-d-PA and its HBr complex are presented.

Thermal Analysis. Figure 8 shows the differential scanning calorimetry **(**DSC) traces obtained for Imi-d-PA (a) and its HBr complex (b). The DSC trace of Imi-d-PA shows a sharp intense endothermic peak at 220 °C upon heating from room temperature to 250 °C at 10 °C/min under N_2 flow, and a low-intensity broad exothermic peak at about 140 °C upon cooling back to room temperature. The thermogravimetric analysis (TGA) trace showed no weight loss up to 240 °C, 3.7% loss from 240 to 395 °C, and extensive thermal degradation above 400 °C (data not shown). The HBr complex showed a sharp intense endothermic peak at 145 °C during heating and no peak upon cooling. Neither material re-crystallizes under the cooling conditions used in the DSC study. We note, however, that there is no hysteresis observed upon heating and cooling of the samples during solid-state ^{1}H NMR studies (300−400 K). In both cases the original spectra are regenerated following the heating sequences. Further DSC studies to investigate the thermal behavior of the materials at high temperatures and on continuous heat−cool cycles would be of interest in considering membrane

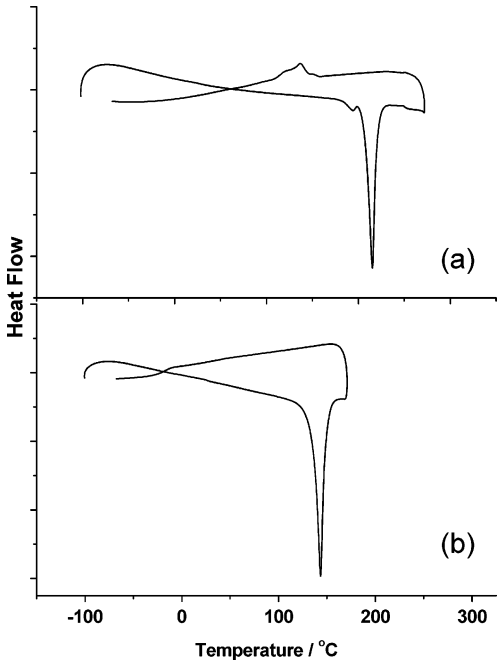

Figure 8. DSC scans of (a) 1,10-(1-*H*-imidazol-5-yl)decanephosphonic acid (Imi-d-PA), T_c peak downward upon heating, peak upward upon cooling, and (b) its HBr complex, 1,10-(1-*H*-imidazol-5-yl)decanephosphonic acid hydrobromide, T_c peak downward upon heating. Data were collected while heating from room temperature to 250 °C at 10 °C/min under N_2 flow.

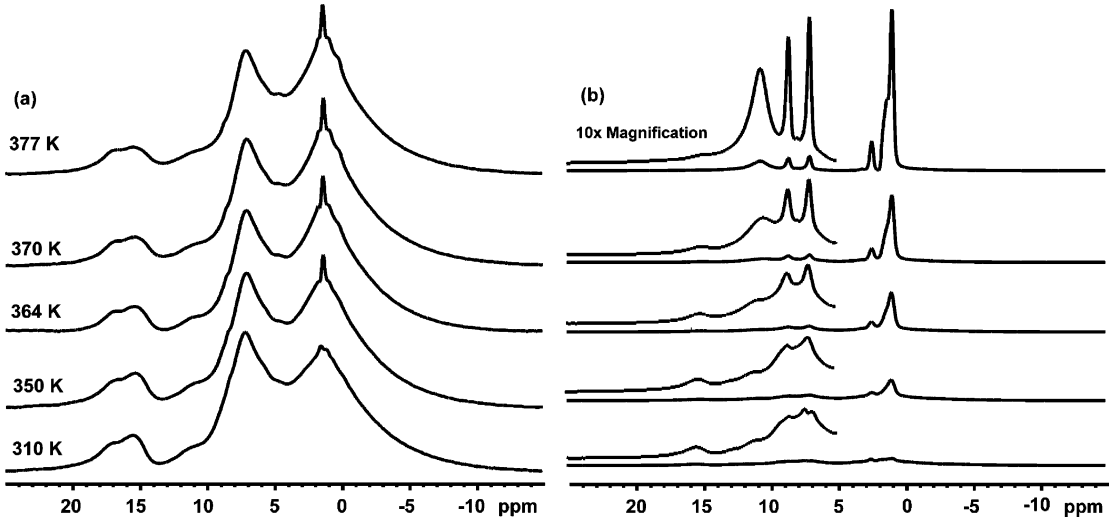

Figure 9. ^{1}H variable temperature NMR spectra acquired at 25 kHz MAS, with sample temperatures ranging from 310 to 377 K. Temperatures are calibrated to take into account the influences of magic angle spinning.[20] (a) Imi-d-PA and (b) Imi-d-PA-HBr. The absence of line narrowing in (a) is attributed to the rigidity of the hydrogen-bonding structure, whereas the onset of coalescence and line narrowing in (b) point to the significant role of the dopant in disrupting the hydrogen-bonding network to allow for local mobility.

longevity and durability, but these are left for another study.

Both materials exhibit a melt transition which is well-defined, indicative of local order or short-range crystallinity. In the case of Imi-d-PA, this melt transition is not reached until 220 °C, whereas in the HBr complex, the melt temperature is reduced by more than 70 °C, to 145 °C. This dramatic lowering of the melt transition is found to be consistent with the proton-transport behavior, investigated by variable temperature ^{1}H NMR below. No glass transition temperature is observed on heating or cooling, but this is not unusual, given the relatively small decane chain, capped with strong H-bond formers. It is also noteworthy that powder diffraction patterns of the materials showed several weak reflections, indicative of polycrystallinity. However, no good quality single crystals were produced. Thus, the combination of thermal analysis and solid-state NMR gives an excellent understanding of the packing constraints and lattice energies of the materials.

Searching for Proton Dynamics. Figure 9a shows the variable temperature ^{1}H MAS spectra acquired for Imi-d-PA, between 310 and 377 K. The surprising observation from this set of data is that no line narrowing occurs in this temperature range. This is in strong contrast to our studies of imidazole-based systems,[6b,d,f] even in the absence of a proton source such as phosphonic acid. From this we conclude that the molecules remain rigid, and moreover, the absence of coalescence, chemical shift changes, or narrowing of the hydrogen-bonded protons (A−D) is a clear indication that these protons are fixed in their positions and unable to contribute to either local proton mobility or long-range proton transport. In parallel with this study, we characterized the HBr-doped analogue of Imi-d-PA. Its hydrogen-bonding structure is quite similar, with resonances B−H apparent in the 1D ^{1}H MAS spectrum. The absence of resonance A indicates that N−H−N bonding is suppressed in the presence of the HBr dopant. The response of this complex to heating, however, is dramatically different than Imi-d-PA itself. As seen in Figure 9b, significant line narrowing in both the aromatic and aliphatic regions of the spectrum are observed as the temperature is increased. The 1D DQF experiment at 370 K shows very poor signal-to-noise (data not shown) and demonstrates both proton and backbone dynamics occur on the time scale of the pulse sequence ($<$20 μs). Aromatic resonances E−F coalesce to a single resonance at 7.0 ppm between 310 and 350 K, indicative of imidazolium ring reorientation. Moreover, the hydrogen-bonded resonances, C−D, coalesce into a single resonance at 10.6 ppm. This is consistent with the weaker nature of these hydrogen bonds relative to the imidazole ring−phosphonate contact of resonance B. Resonance B does not coalesce in this temperature range, but does tend toward lower frequency, consistent with weakening or more dynamic hydrogen bonding.

From these results, we propose that the rotation of the phosphonate group is the more energetically-efficient step in proton transport, whereas the ring reorientation of the imidazole rings are more energetically costly. Moreover, when there are no excess protons, as in the undoped Imi-d-PA material, no proton transport occurs, due to the high lattice energy associated with the fully hydrogen-bonded network. When the system is doped with HBr, the protonated imidazolium rings and/or phosphonate units become loosely bonded to neighboring groups and are able to pass on their protons. This is favored in the phosphonate centers over the imidazolium units, as indicated by the varying H-bonding strengths assigned based on the magnitude of the proton chemical shift, and the earlier onset of coalescence among resonances C−D.

It is very informative to compare these results for local proton dynamics in Imi-d-PA with macroscopic impedance measurements of the related copolymer, poly(VPA-*co*-4-VIm).[8] This copolymer is an analogue of the Imi-d-PA studied here. It incorporates VPA as a proton source and 4-VIm as a proton solvent. It was confirmed that the imidazole rings were protonated and that dc conductivites of the dry copolymers were between 10^{-6} and 10^{-12} S/cm. Proton conductivity by vacancy migration, attributed to structural diffusion, was deduced. The extremely low con-

ductivity of these polymers fits well with the observations made for Imi-d-PA on the molecular scale. Protons are not sufficiently mobile in either case to give rise to long-range proton transport under dry conditions. With the addition of HBr as a dopant, additional protons are available for conductivity, and moreover, the hydrogen-bonding network is interrupted by these dopant ions, providing a lowering of the lattice energy to facilitate structural diffusion. Our results can therefore be generalized to conclude that polyelectrolytes which provide 1:1 ratios of proton solvent to proton source, where both solvent and source are covalently tethered to the polymer backbone, are as yet not successful proton-conducting membranes under dry conditions. Although we leave the door open to further synthetic developments, we note that these results indicate a fundamental cooperativity between structural and vehicular proton diffusion, where high rates of proton transport are prohibited in the absence of a vehicular-transport option, be it a water molecule or an acid dopant.

Conclusions

High-resolution solid-state ^{1}H NMR achieved under fast magic angle spinning (60 kHz MAS) together with multidimensional heteronuclear correlation spectroscopy were used to establish the hydrogen-bonding structure and probe proton dynamics in 1,10-(1-*H*-imidazol-5-yl)decanephosphonic acid and its HBr-doped counterpart. The hydrogen-bonding motif in Imi-d-PA was found to incorporate four types of hydrogen bond, including ring−ring bonds between imidazole rings, P−O−H−O−P bonds among phosphonate groups, and two types of phosphonate−imidazole ring bonds, differentiated according to the asymmetric bonding around the imidazole rings. This network of hydrogen bonds, however, was found to be unable to transport protons, as found by variable temperature ^{1}H NMR studies. In contrast, the HBr-doped Imi-d-PA material demonstrated significant proton mobility, and overall molecular dynamics, the essential molecular level processes which enable proton transport.

Experimental Section

1,10-(1-*H*-imidazol-5-yl)decane (diethyl)phosphonate (Im-CH_2-$(CH_2)_8CH_2$-PO_3Et_2) was obtained as previously reported; synthetic details can be found in the literature.[9] This compound was taken up with excess concentrated HBr and refluxed 24 h. Afterward HBr was vacuum-evaporated. The residue was taken up with EtOH, dried under vacuum, washed with CH_3CN, and filtered. The filtered solid was taken up again with EtOH. The solid hydrobromide of 1,10-(1-*H*-imidazol-5-yl)decanephosphonic acid precipitated from this solution upon slow evaporation of the solvent at room temperature. This material was dried under vacuum at room temperature to constant weight. This material, the Imi-d-PA HBr complex, was kept dry and used for solid-state NMR and DSC studies.

The hydrobromide was taken up with water to yield a suspension. An equimolar amount of solid NaOH was added under stirring to this suspension to neutral pH. The solid was filtered, washed with MeOH, and dried at room temperature under vacuum to yield 1,10-(1-*H*-imidazol-5-yl)decanephosphonic acid, Imi-d-PA. This material was also kept dry and used for solid-state NMR and DSC studies.

The conditions of the cross-polarized MAS (CP-MAS) NMR experiments are described below and were collected using a MAS frequency of 25 kHz with a double-resonance probe using rotors with a 2.5-mm outer diameter. The various 2D spectra were collected on a Bruker Avance 500 with a proton Larmor frequency of 500.13 MHz and the proton chemical shift was referenced to adamantane protons which have a chemical shift of 1.63 ppm. The carbon Larmor frequency is 125.76 MHz and was referenced to the carbonyl in the α-polymorph of glycine at 176.14 ppm. The ^{1}H−^{13}C CPMAS spectra were collected at contact times of 0.5 ms, 3 ms, and 6 ms. All spectra utilized a proton 90° pulse length of 3.5 μs, a recycle delay of 2 s, and a bearing gas temperature of 300 K. The shortest contact time required 4000 transients, whereas the longer contact times were collected with 2000 transients. The ^{1}H−^{31}P CP-MAS spectrum used a ^{31}P Larmor frequency of 202.45 MHz and was referenced to phosphoric acid at 0.0 ppm. The spectrum was collected using 256 transients with a contact time of 3000 μs and a proton 90° pulse of 2.5 μs, a recycle delay of 2 s, and a bearing gas temperature of 300 K.

The ^{1}H MAS NMR and BaBa experiments were conducted on a Bruker AMX 600 with a proton Larmor frequency of 600.16 MHz. The probe used was a single-resonance prototype that supported rotors with a diameter of 1.1 mm, capabable of achieving MAS spinning speeds of 70 kHz. Spectra reported here were acquired at 60 kHz MAS, using a gas cooling line which controlled the sample temperature to roughly 15 °C above ambient temperature. The 1D ^{1}H MAS experiments were collected with 64 transients. The rotor-synchronized 2D ^{1}H−^{1}H BaBa spectra were collected with $\tau_{exc} = 2\tau_r$ and 800 transients.

DSC data were acquired with a Mettler TA 3000 instrument coupled to a Mettler TC10A TA microprocessor, operated in N_2 at 10 °C/min.

Acknowledgment. The authors are grateful to Alex Bain for insightful reviews of the manuscript. This research was supported by an NSERC Discovery grant to G.R.G. A.S. and co-workers are grateful to the Estonian Science Foundation for financial support.

CM060514I